CrossMark

RESEARCH ARTICLE

Slow-release formulations of the herbicide picloram by using Fe–Al pillared montmorillonite

Jose L. Marco-Brown[1,2,3] · Tomás Undabeytia[4] · Rosa M. Torres Sánchez[5] · María dos Santos Afonso[1,2]

Abstract Slow-release formulations of the herbicide picloram (PCM, 4-amino-3,5,6-trichloropyridine-2-carboxylic acid) were designed based on its adsorption on pillared clays (pillared clays (PILCs)) for reducing the water-polluting risk derived from its use in conventional formulations. Fe–Al PILCs were synthesized by the reaction of Na^+-montmorillonite (SWy-2) with base-hydrolyzed solutions of Fe and Al. The Fe/(Fe + Al) ratios used were 0.15 and 0.50. The PCM adsorption isotherms on Fe–Al PILCs were well fitted to Langmuir and Freundlich models. The PCM adsorption capacity depended on the Fe content in the PILCs. Slow-release formulations were prepared by enhanced adsorption of the herbicide from PCM-cyclodextrin (CD) complexes in solution. CDs were able to enhance up to 2.5-fold the solubility of PCM by the formation of inclusion complexes where the ring moiety of the herbicide was partially trapped within the CD cavity. Competitive adsorption of anions such as sulfate, phosphate, and chloride as well as the FTIR analysis of PCM-PILC complexes provided evidence of formation of inner sphere complexes of PCM-CD on Fe–Al PILCs. Release of the herbicide in a sandy soil was lower from Fe–Al PILC formulations relative to a PCM commercial formulation.

Introduction

A great variety of pesticides (herbicides, insecticides, fungicides) (Akelah 1996; Delcour et al. 2015; Kenawy et al. 1992; Qi & Donahoe 2008) have been produced and used in the last 50 years, aiming to protect and to increase the yield of agri-

Responsible editor: Guilherme L. Dotto

✉ Jose L. Marco-Brown
josemarcobrown@gmail.com; joseluis.marcobrown@unsam.edu.ar

Tomás Undabeytia
undabeyt@irnase.csic.es

Rosa M. Torres Sánchez
rosats@cetmic.unlp.edu.ar

María dos Santos Afonso
dosantos@qi.fcen.uba.ar

[1] Departamento de Química Inorgánica, Analítica y Química Física, Facultad de Ciencias Exactas y Naturales, Universidad de Buenos Aires, Ciudad Universitaria, Pabellón II, C1428EHA Buenos Aires, Argentina

[2] Instituto de Química Física de los Materiales, Medio Ambiente y Energía de la Facultad de Ciencias Exactas y Naturales (INQUIMAE), CONICET-Universidad de Buenos Aires, Buenos Aires, Argentina

[3] Present address: Instituto de Investigación e Ingeniería Ambiental (3iA), CONICET, Escuela de Ciencia y Tecnología, UNSAM, 25 de Mayo y Francia (1650), San Martín, Argentina

[4] Institute of Natural Resources and Agrobiology (IRNAS-CSIC), Reina Mercedes 10. Apdo. 1052, 41080 Sevilla, Spain

[5] Centro de Tecnología en Recursos Minerales y Cerámica (CETMIC), CONICET-CCT La Plata-CIC, Camino Centenario y 506 CC (49), B1897ZCA M. B. Gonnet, Argentina

2 Springer

cultural production. Usually, pesticides are sprayed as fine particles suspended in aqueous media or, in some cases, in the presence of organic compounds to form aqueous emulsions that offer a good contact surface with the crop. The excess of pesticide, non-absorbed by crops, is partially vaporized to the atmosphere and also leached below root zone by rain or irrigation. These losses in the amount of the applied pesticide would reach and contaminate groundwater and/or surface water bodies (Haynes et al. 2000; Loewy et al. 1999; Schipper et al. 2008). To minimize this effect, in the last decades, research has focused on the development of slow-release formulations (SRFs) of herbicides. SRF of fertilizers had been studied too in order to reduce the contamination by nitrogen and phosphorous (Entry & Sojka 2008). The benefits in using SRFs are follows: increased availability of pesticides in order to enhance the desired control of the crop, reduction of the frequency of application and leaching of the pesticide in the soil, and therefore the risk of groundwater contamination (Maqueda et al. 2008; Undabeytia et al. 2010).

The low cost and easy access to natural inorganic materials such as clay minerals have allowed their use as adsorbents and also as SRFs (Ali et al. 2012; Carrizosa et al. 2000; Galán-Jiménez et al. 2013; Gupta and Suhas 2009; Lagaly 2001; Sánchez-Jiménez et al. 2012). Montmorillonite (Mt) has relevant properties as its high surface area and laminar structure that make it an excellent matrix to attach different chemical species to generate SRF systems: clay protein composites (Alromeed et al. 2015), phosphatidylcholine vesicles adsorbed on clay (Undabeytia et al. 2011; Undabeytia et al. 2012), alginate/exfoliated Mt nanocomposite (Yan et al. 2015), etc. In the design of SRFs, the use of polysaccharides (Campos et al. 2014), chitosan (Kashyap et al. 2015), sepiolite gels (Maqueda et al. 2008, 2009), and herbicide encapsulation by poly(butyl acrylate-co-styrene) (Wang et al. 2015) have been also proposed.

Pillared clay (PILC) minerals have been used as catalysts, adsorbents for the removal of pollutants, and SRFs, due to its multiple loaded centers, large area, high thermal stability, and interlayer space. Particularly, Fe-PILCs were used for preparation of SRFs of the herbicide imazaquin (Undabeytia et al. 2013).

Picloram, 4-amino-3,5,6-trichloropyridine-2-carboxylic acid (PCM) is a synthetic organic chemical that belongs to the pyridine family. This organic compound has herbicide activity and is used to control annual broad leaf weeds at low rates and deeply rooted herbaceous weeds, in vines, woody plants, and cereals crops such as wheat, barley, and oats (FAO 2007; Palma et al. 2004). Kinetic and equilibrium processes of PCM adsorption on Mt and Fe PILC have been previously reported (Marco-Brown et al. 2014; Marco-Brown et al. 2012), with a greater adsorption capacity on Fe PILC. With both clays, the adsorption of PCM on the mineral surfaces occurred between the pyridine and carboxylate functional moieties of groups in the PCM molecule and the metal

centers at the mineral surface (Marco-Brown et al. 2015). PCMs at the pH of most of the soils and water environments (pKa ≈2.3) present a very low adsorption on soil particles and extremely high soil mobility (Biggar et al. 1978; Celis et al. 2002; Cheung & Biggar 1974; Hall et al. 2015; Osteryoung & Whittaker 1980). Therefore, it would be of interest to obtain SRF of this herbicide based on modified clays such as PILCs to minimize its environmental pollution.

In general, the active ingredient loading on clay-based formulations is limited by the herbicide solubility, which prevents further adsorption (Undabeytia et al. 2013). Cyclodextrins (CDs) are cyclic oligosaccharides obtained from the enzymatic degradation of starch and formed by 6 to 12 units of α-D-glucopyranose linked through bonds α $(1 \rightarrow 4)$. CDs are crystalline, highly soluble in water with a conformation of a truncated cone with a cavity therein (Szejtli 1998). This cavity is hydrophobic, because the methylene hydrogen atoms and glycosidic oxygen atoms are located inside the cavity, whereas its outer surface is hydrophilic due to the hydroxyls 2, 3, and 6 of the glucanopyranose molecules. These features give to the CDs the ability to accommodate organic molecules as guest molecules in its interior, forming inclusion complexes, thus favoring the water solubility of the host. The CD inclusion complex formation is a dynamic equilibrium process. CDs have been deeply investigated for their use as drug delivery systems, sequestering agents, solubility increase of compounds in aqueous solution, and soil remediation (Jozefaciuk et al. 2001; Morillo et al. 2014; Undabeytia et al. 2013; Wenz et al. 2006; Yáñez et al. 2012).

In this study and due to the great sorption capacity of Fe PILC for PCM previously evidenced (Marco-Brown et al. 2012), the use of CDs for enhanced solubility of the herbicide PCM will be explored with the aim of increasing the active ingredient content in PILC-based SRFs.

The aims of this work are (i) to evaluate PCM adsorption on Fe–Al PILCs for the preparation of SRFs, (ii) to study the solubility enhancement in water of PCM by the use of CDs, (iii) to evaluate PCM adsorption on Fe–Al PILCs in the presence of CDs and compare with PCM adsorption without CDs, (iv) to get insight into the mechanisms involved in the preparation of the SRFs, and finally (v) to test these formulations for slow release.

Materials and methods

Materials

Wyoming Na-Mt (SWy-2) was obtained from the Source Clays Repository of The Clay Minerals Society (Columbia, MO) (cation exchange capacity 0.8 mmol/g). Al(NO$_3$)$_3$·9H$_2$O, FeCl$_3$·6H$_2$O, NaCl, Na$_2$SO$_4$, Na$_3$PO$_4$, H$_3$PO$_4$, and NaOH were purchased from Sigma-Aldrich (Sigma Chemical Co., St. Louis, MO). HPLC-grade acetonitrile was obtained from

Teknokroma S.A. (Barcelona, Spain). Picloram (PCM 100% purity) was supplied by Sigma-Aldrich. The commercial formulation of PCM (Tordon® 101) was supplied by PRINA AGROTÉCNICA, S.L. (Sevilla, Spain). Cyclodextrins (CDs) were purchased from Cyclolab (Budapest, Hungary). The CDs employed were α-CD, β-CD, hydroxypropyl-β-CD (HPβ), and randomly methylated β-CD (RAMEβ). Figures 1 and 2 show the structural formulas of PCM and CDs, respectively.

Soil samples were collected from the Ap Horizon (0–20 cm) of a sandy soil (SS) classified as Typic Xeropsamment. These soil samples were passed through a 2-mm sieve before use in PCM release studies. This soil has a pH 8.9 and 0.79% of organic matter content (more detailed physicochemical properties were reported by Undabeytia et al. 2012).

Pillared clay mineral synthesis

Synthesis of PILC mineral was done as reported elsewhere (Undabeytia et al. 2013). Briefly, aluminum nitrate and iron chloride solutions in two Fe/(Fe + Al) molar ratios (0.15 and 0.5) were hydrolyzed by titration with 0.4 M NaOH under nitrogen atmosphere. The Al/OH molar ratio was 2.0. These pillaring solutions were aged for 7 days. Then, 10 g of clay mineral was dispersed in 250 mL water, and the pillaring solutions were added slowly at a ratio of 10 mmol (Fe + Al)/g clay mineral with a peristaltic pump under nitrogen atmosphere. The final clay mineral content was 1% (w/w). The dispersions were shaken for 24 h, followed by centrifugation, removal of chloride anions by dialysis, dry freezing, and further heating at 300 °C under nitrogen atmosphere. The products were identified as P0.15 and P0.5 samples, where the numbers indicated the Fe/(Fe + Al) molar ratio used. The interlayer spaces for P0.15 and P0.5 were determined to be 0.9 and 4.3 nm, respectively, by X-ray diffraction (XRD) (Undabeytia et al. 2013). Nitrogen adsorption-desorption isotherms (see Fig. S1 in Supplementary Material) were recorded at 77 K using a Micromeritics ASAP 2010 instrument. P0.15 and P0.5 presented a type II nitrogen adsorption-desorption isotherms (Fig. S1) with a type H3 hysteresis typically associated with materials formed by sheet agglomerations of lamellar particles yielding mesopores and macropores.

Surface areas determined were 195 and 172 m²/g for P0.15 and P0.5, respectively (Undabeytia et al. 2013). Scanning
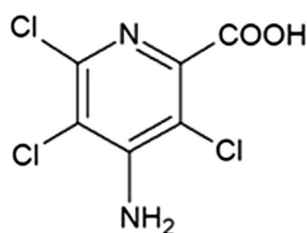

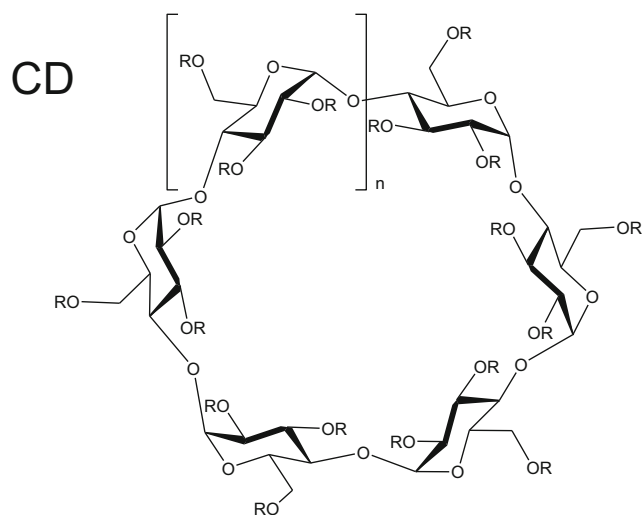Fig. 1 Structural formula of picloram (PCM)

Fig. 2 Structural formula of cyclodextrins (CDs). α-CD, $n = 1$, R = H; β-CD, $n = 2$, R = H; HP-β, $n = 2$, R = H or CH_2-CHOH-CH_3 and RAMEβ, $n = 2$, R = H or CH_3

electron microscopy (SEM) was performed using a file emission gun scanning electron microscope Zeiss (FEG-SEM Zeiss LEO 982 GEMINI) with combined energy-dispersive X-ray (EDS) analyzer. The SEM images were taken by applying 3 kV voltage with 4000 times magnification for the clarification of surface. The surface morphology of the clay surface changed after pillaring to a more porous and fluffy appearance as the iron content increased revealing coaggregation of iron polyoxocations on the clay mineral surface as noticed by EDS (see Fig. S2 in Supplementary Material).

Adsorption studies

PCM adsorption experiments were performed in duplicate by mixing 24 mg of the PILC with 15 mL of PCM solutions ranging up to 1.66 mM. Preliminary kinetic studies indicated that adsorption reached equilibrium after 24 h; thus, the dispersions were shaken for 24 h at 20 °C. Subsequently, the dispersions were centrifuged and the concentration of herbicide in the supernatants was determined.

PCM adsorption on P0.5 was also done in the presence of RAMEβ and HPβ. For these experiments, 24 mg of P0.5 was suspended in 15 mL of a solution of PCM and CD. Molar ratios of 4.97:100 for PCM/RAMEβ and 3.93:100 for PCM/HPβ were used respectively.

Adsorption of PCM on P0.5 was also studied in the presence of NaCl, Na_2SO_4, and Na_3PO_4 electrolytes. Typically, 24 mg of PILC was mixed in a 1.66 mM PCM solution with a molar ratio of 1:1 PCM/electrolyte.

The PCM concentration was determined by a Shimadzu HPLC equipped with PDA detector set at a wavelength of 230 nm. An injection volume of 100 μL was used. The mobile phase was a mixture of 50% acetonitrile and 50% water containing 1% acetic acid. A C18 reverse-phase column

(Kromasil 100, 150-mm length, 0.5-mm internal diameter) was used. The flow rate was 1 mL/min. PCM retention time was 1.5 min. The adsorption experiments were performed in duplicate. The standard error was always lower than 5%.

Experimental data for PCM adsorption were analyzed using Langmuir and Freundlich models.

Langmuir adsorption isotherms

The Langmuir model is used frequently to explain adsorption processes. This model assumes a reduction of the available interaction places as the adsorbate concentration increases. The Langmuir isotherm assumes monolayer adsorption and is represented by the following equation:

$$\Gamma = \frac{\Gamma_{max} K_L C_{eq}}{\left(1 + K_L C_{eq}\right)} \tag{1}$$

where Γ_{max} is the maximum uptake and means the maximum concentration on the solid phase, C_{eq} is the adsorbate concentration at the equilibrium on the aqueous media, and K_L is the Langmuir equilibrium constant, which is related with the free energy of the reaction.

Freundlich adsorption isotherms

The Freundlich isotherm is an empirical equation that describes the adsorption on a heterogeneous surface with a non-uniform distribution of heat of adsorption that means that the surface on which the adsorbed molecules are interacting is energetically heterogeneous. This model does not predict any saturation of the adsorbent by the sorbate. Instead, infinite surface coverage is predicted, indicating multilayer adsorption on the surface. This isotherm is determined by the following equation:

$$\Gamma_e = K_F \times C_{eq}^{1/n} \tag{2}$$

where K_F is the Freundlich constant indicating adsorption capacity and represents a measure of the surface area of the adsorbent while $1/n$ is an irrational fraction that varies between 0.1 and 1 and is a measure of the adsorption intensity.

PCM solubility studies in aqueous phase in the presence of CD

Due to the low solubility of PCM in water, a solubility study in presence of CD was done. PCM (20 mg) was added in excess of its solubility at 25 °C (430 mg/L) to aqueous solutions (10 mL) containing various concentrations of each CD. The concentration range was from 0 to 16 mM for β-CD and from 0 to 100 mM for α-CD, HPβ, and RAMEβ. CD solutions were previously prepared in order to obtain the desired concentrations and sonicated. The experiments were carried out in triplicate. Flasks containing

the dispersions were sealed and shaken for 1 week. This reaction time was chosen after preliminary kinetic studies (data not shown). The dispersions were left to settle down for 24 h, and aliquots from the supernatants were then filtered using a syringe through a 0.22-μm Millipore cellulose glass fiber membrane filter, and the concentration of PCM in the filtrate was determined by HPLC. For the calculations, as will be seen later, only the total CD concentration used as well as PCM concentration in the filtrates was needed.

PCM formulation preparation

Two formulations were prepared by adsorption of PCM and PCM-HPβ complexes on P0.5 at 1.6 g clay/L. One formulation was prepared by mixing 24 mg of P0.5 with 15 mL of 1.66 mM PCM solution. The other one was prepared in the same way, mixing 24 mg of P0.5 with 15 mL of a solution containing PCM and HPβ with concentrations of 2.90 and 73.69 mM, respectively.

The dispersions were shaken for 24 h at 20 °C. Then, the herbicide was analyzed in the removed supernatant, whereas the pellets were dry-frozen yielding the PILC formulations. They were denoted as PCM-P0.5 and PCM-HPβ-P0.5. The contents of PCM in PCM-P0.5 and PCM-HPβ-P0.5 formulations were 5.7 and 7.6% w/w, respectively.

Characterization of the adsorbent, adsorbates, and adsorption products

Fourier-transform infrared (FTIR) spectra of P0.5, PCM, HPβ, PCM-HPβ complex, PCM-HPβ(PM) samples, and PCM-P0.5 and PCM-HPβ-P0.5 formulations were recorded on a FTIR Nicolet 8700 spectrometer equipped with a DTGS detector, using KBr discs, scanned in a wave number range of 400–4000 cm^{-1}. The PCM-HPβ complex was obtained by dry-freezing a solution of PCM 2.5 mM and HPβ 5.5 mM previously shaken at 20 °C during 24 h. The physical mixture of PCM and HPβ denoted as PCM-HPβ(PM) was prepared by grinding in a mortar PCM and HPβ at a 1:1-M ratio.

Release of herbicide

The release of PCM from prepared formulations PCM-P0.5 and PCM-HPβ-P0.5 and a commercial formulation (Tordon® 101) were conducted by using Büchner funnels. In this procedure, 98.9 g of sandy soil (SS) was added to a Büchner funnel (70.88 cm^2 of surface area) equipped with a paper filter on the bottom. The soil sample was homogenized to a 0.5 cm height. The herbicide formulations were uniformly spread over the soil at a rate of 2.0 kg of active ingredient (a.i.) per hectare. The soil samples in each funnel were irrigated 15 times with 15 mL, each washing corresponding to 2.12 mm rain at 20 min intervals. The eluted volume after each watering was

collected, and the concentration of herbicide in the eluent was determined by HPLC. All experiments were carried out by triplicate.

Results and discussion

PCM adsorption on PILCs

PCM adsorption isotherms on P0.5 and P0.15 are depicted in Fig. 3. Adsorption coverage (Γ_{ads}) of PCM on P0.5 was about 4-fold higher than that found on P0.15. This adsorption increase can be ascribed to the surface site modifications originated by the iron pillaring process. In the development of PILC minerals with mixed oxides, the properties of the product depended on the iron content in the structure. In this sense, it was reported an increment in the trichloroethylene oxidation capacity by the use of a PILC (Mishra et al. 2008) and also an increase in the herbicide imazaquin adsorption capacity of Fe–Al PILC related to the structural Fe content (Undabeytia et al. 2013). The latter authors explained that the high affinity of the herbicide to iron surface sites yielded an increase in imazaquin adsorption. Moreover, a Γ_{ads} increase for PCM adsorption on a Fe pillared Mt relative to a raw Mt was also found (Marco-Brown et al. 2012).

The adsorption isotherms are important criteria in the optimization of the use of adsorbent materials, because the correlation between experimental data and adsorption models may be related to different interactions (binding strength, heterogeneity/homogeneity of adsorbent sites, adsorbate monolayer formation, etc.) between sorbate and adsorbent. Thus, analysis of experimentally obtained equilibrium data by either theoretical or empirical equations is useful for the practical design of adsorption systems aimed at slow release. Consequently, experimental data for PCM adsorption were analyzed using both Langmuir and Freundlich models.

The experimental data were well fitted to the Langmuir and Freundlich models (Fig. 3 and Table 1). In the Langmuir
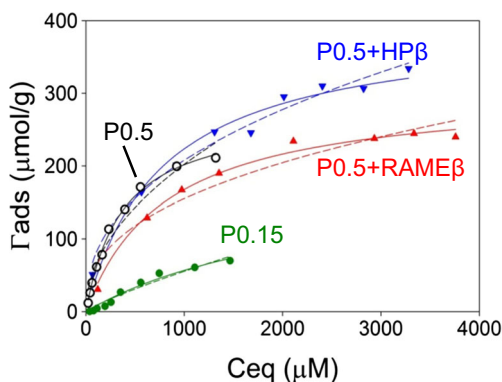

Fig. 3 PCM adsorption isotherms on P0.15 (*green circles*), P0.5 (*white circles*), P0.5 (*red triangles*) in the presence of RAMEβ, and P0.5 (*blue inverted triangles*) in the presence of HPβ. *Solid* and *dashed lines* represent Langmuir and Freundlich fits, respectively

model, the affinity between sorbent and sorbate is represented by the constant K_L. In general, for good sorbents, high Γ_{max} and K_L are desirable.

The K_L for PCM sorption on P0.5 is within the range of values reported for strong interactions of organic molecules on clays: benzyltrimethylammonium on Mt (5000 M^{-1}) (Nir et al. 2000) and ethoxylated alcohols on sepiolite (680–900 M^{-1}) (Galán-Jiménez et al. 2013). In the particular case of PILCs, the existence of strong Brönsted and Lewis acid centers can promote the formation of inner sphere complexes with the loaded metal centers on the clay. No conclusion may be achieved by the examination of the K_L value of PCM. A higher K_L value than that of PCM was obtained for the sorption of the anionic herbicide sulfometuron on PILC (12,000 M^{-1}), whose sorption mechanism was only dominated by strong electrostatic interactions (Nir et al. 2000).

Solubility diagrams of PCM in the presence of CDs

The evaluation of PCM water solubility in the presence of β-CD, α-CD, HPβ, and RAMEβ indicated an increase with CD concentration due to the formation of an inclusion complex picloram-cyclodextrin (PCM-CD) (Fig. 4). In this PCM-CD complex, part of the ring of the herbicide molecule was trapped in the polar cavity of CD. The increase of PCM solubility with CD concentration as noticed with β-CD, HPβ, and RAMEβ indicated the existence of an inclusion complex without a solubility limit (Higuchi & Connors 1965; Undabeytia et al. 2013). According to Higuchi & Connors (1965), these solubility diagrams correspond to the formation of an inclusion complex with a 1:1 stoichiometry. However, when α-CD was used, PCM solubility decreased after a 70 mM α-CD concentration, indicating a complex solubility limit above which the complex precipitated.

The inclusion complex formation is a dynamic equilibrium process (Higuchi & Connors 1965) and can be expressed by the following equation:

$$m\,S + n\,L \xleftrightarrow{K_{m:n}} S_m L_n \tag{3}$$

where S is the adsorbate (PCM), L is the ligand (CD), $S_m L_n$ is the inclusion complex, and $K_{m:n}$ is the apparent stability constant of the inclusion complex and can be calculated by the following equation:

$$K_{m:n} = \frac{[S_m L_n]}{[S]^m [L]^n} \tag{4}$$

where $[S] = S_0$, $[L] = L_t - n[S_m L_n]$, $[S_m L_n] = (S_t - S_0)\,/\,m$, S_0 is the adsorbate concentration in the absence of ligand L and in the presence of solid PCM, that is, the water solubility of S, S_t is the adsorbate concentration in solution, and L_t is the total concentration of ligand added to the system. Combining these

Table 1 Langmuir and Freundlich parameters for PCM adsorption onto P0.15 and P0.5 samples in presence and absence of CDs

Adsorbent	Langmuir			Freundlich		
	K_L (M^{-1})	Γ_{max} (mol/kg)	R^2	K_F	$1/n$	R^2
P0.15	410	0.19	0.9677	6.45	0.50	0.9570
P0.5	1460	0.37	0.9794	5.64	0.52	0.9728
P0.5 + RAMEβ	1460	0.29	0.9862	9.97	0.40	0.9253
P0.5 + HPβ	1460	0.38	0.9714	15.49	0.38	0.9725

equations and applying them to known concentrations ($n = 1$ and $m = 1$) lead to the following expression:

$$S_t = S_0 + \frac{K_{1:1}S_0L_t}{1 + K_{1:1}S_0} \tag{5}$$

By plotting S_t vs L_t, a straight line with intercept equal to S_0 is obtained, where the slope is defined by Eq. 6:

$$\text{slope} = \frac{K_{1:1}S_0}{1 + K_{1:1}S_0} \tag{6}$$

Therefore, as stated earlier, the stability constant is given by Eq. 7:

$$K_{1:1} = \frac{\text{slope}}{S_0(1-\text{slope})} \tag{7}$$

The graphical representation of PCM solubility (S_t) as a function of the added CD (L_t) gave a straight line in accordance to the mechanistic formation of a 1:1 PCM/CD complex (Fig. 4). In particular, the rising part of the solubility curve of PCM with α-CD was used for the calculation of K_c (Eq. 7). K_c values obtained for the PCM-CD complexes using β-CD, α-CD, HPβ, and RAMEβ CDs are shown in Table 2. The fitting was reasonably good, especially for RAMEβ and Hβ-CDs. The type of diagram found for α-CD can also indicate the formation of a more complex stoichiometry (Pérez-Martínez et al. 2000). In this case, a larger deviation in the goodness of
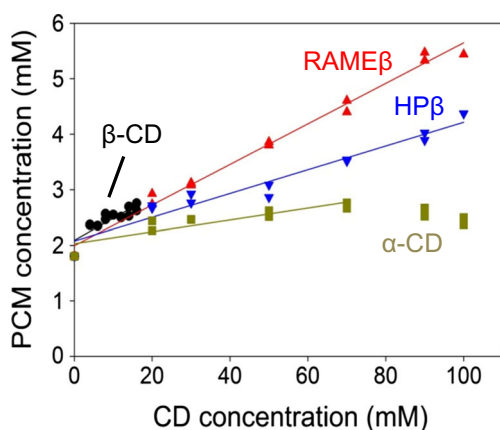
the fit would have been noticed; however, a similar R^2 value to that of β-CD was obtained.

Solubility efficiency (S_e) was also obtained from the solubility diagrams (Table 2), which is defined as the increment in the apparent solubility of PCM at a fixed CD concentration with respect to its solubility in the absence of CD. The inclusion complex of PCM with β-CD had the highest K_c value; however, due to the lower solubility of β-CD, the total concentration of solubilized PCM after the addition of β-CD was low compared to that reached with the addition of HPβ or RAMEβ. The maximal increment in PCM solubility occurred with RAMEβ (up to 2.5-fold). The enhanced solubility of the herbicide was also remarkable with HPβ, with solubility increments up to 2-fold. The percentage of encapsulation efficiency (E_{encap}) of PCM in CDs was obtained as $[S_mL_n] \times 100/L_t$ at a fixed CD concentration (Table 2). In general, low encapsulation efficiency was obtained for the whole CDs evaluated.

PCM adsorption on PILC in the presence of CDs

In the synthesis of delivery or slow-release materials, it is desirable to make that the content ratio of active ingredient/formulated mass has an appropriate value to the purpose thereof.

In the preparation of SRFs based on Al–Fe PILC minerals, the a.i. content of the formulation may be optimized by the use of ligands such as CDs that enhance the solubility of the herbicide in solution and on its turn permit to increase its sorption on the clay matrix.

Fig. 4 Solubility diagrams of picloram in aqueous solutions in the presence of CD: β-CD (*black circles*), RAMEβ (*red triangles*), HPβ (*blue inverted triangles*), and α-CD (*green squares/rectangles*)

Table 2 Apparent stability constants (K_c), regression coefficients (R^2), solubility increase (S_e, using 0–0.016 M for β-CD and 0–0.1 M for the other CD), and efficiency of encapsulation (E_{encap}) for the inclusion compounds obtained between picloram and the different CDs

Parameter	RAME β-CD	HPβ-CD	α-CD	β-CD
K_c (L/mmol)	1.90×10^{-2}	1.05×10^{-2}	5.28×10^{-3}	1.97×10^{-2}
S_e	2.65	2.13	1.35	1.34
E_{encap} (%)	3.8	2.3	1.0	4.4
R^2	0.9880	0.9437	0.8086	0.7305

K_c is calculated based on the concentration of the species in equilibrium and not in terms of activities, which is indicated by the units in parentheses

This approach was tested with the PILC mineral P0.5 in the presence of RAMEβ and HPβ CDs, which turned out to be the most effective for maximizing the concentration of PCM solution. The choice of P0.5 as adsorbent material was based on its higher sorption capacity (Fig. 3).

The PCM adsorption isotherms on P0.5 in the presence of RAMEβ and HPβ obtained are shown in Fig. 3, as well as the fit of the experimental data by adsorption models of Langmuir and Freundlich. The values of the fitting parameters to the experimental data of PCM adsorption isotherms on P0.5 in the presence of RAMEβ and HPβ obtained from modeling by Langmuir and Freundlich are listed in Table 1.

With the Langmuir model, the coincidence of K_L value obtained for PCM adsorption on P0.5 in the absence of CDs with that in the presence of RAMEβ and HPβ ($1460 M^{-1}$) indicated that CDs did not modify the mechanism of PCM interaction with the surface of the PILC mineral.

The maximum coating Γ_{max} increased slightly from 0.37 to 0.38 mol/kg, in presence of HPβ. These results also pointed that the presence of HPβ only increased the PCM concentration in solution but without participating in the adsorption process, achieving higher Γ_{ads} values than in the absence of CD.

The maximum coating Γ_{max} value was about 30% lower in the presence of RAMEβ than in the presence of HPβ (Fig. 3 and Table 1). This result may indicate that the RAMEβ CD was adsorbed onto the adsorbent surface, which resulted by either the competition with the PCM and occupation of the same sites or by steric hindrance preventing the PCM access to adsorption sites of the PILC. A RAMEβ strong interaction with bentonite, illite, and kaolinite clay mineral surfaces was reported (Jozefaciuk et al. 2001), causing a decrease in surface area of the micropores and mesopores.

From the Langmuir constant value K_L, the standard free energy adsorption process was calculated $\Delta G° = −18 kJ mol^{−1}$, which is an indicative of a spontaneous adsorption process.

These results indicated that the use of CDs enhanced the PCM solubility increasing its maximal adsorbed amount on P0.5 by the use of HPβ. Therefore, the use of HPβ is recommended in the preparation of PCM-Al–Fe PILC formulations.

PCM adsorption in the presence of electrolytes

The use of HPβ increased PCM sorption on P0.5, but it did not affect the mechanisms involved on its sorption on the clay because the analysis of the K_L values showed identical affinity. Then, the only function of this CD was to enhance the solubilization of the herbicide by the formation of an inclusion complex, which is followed by its disruption and sorption of PCM. To elucidate the mechanisms involved on PCM sorption on P0.5, a study was performed in presence of competitive anions whose

interaction modes with PILC were previously established. No influence of the HPβ presence is expected, and for simplicity, this analysis was performed with PCM solutions in the absence of HPβ.

PCM adsorption on P0.5 sample in the presence of chloride, sulfate, and phosphate anions was also studied (Fig. 5). The presence of chloride ions did not change the amount of PCM adsorbed while the presence of sulfate and phosphate anions decreased drastically the adsorption of the herbicide.

Adsorption from strong anions such as $Cl^−$, $NO_3^−$, $Br^−$, and $ClO_4^−$ to functional groups on the surface of mineral acids occurs through outer sphere complexation processes driven mainly by electrostatic forces (Essington 2004).

The adsorption of phosphate ions on metal oxides has been reported to occur by inner sphere complexation processes, interacting with a metal center via formation of monodentate or bidentate complexes or with two adjacent metal centers by forming a bridge complex (He et al. 1997; Higuchi & Connors 1965).

On the contrary, the adsorption of sulfate anions on mineral surfaces such as γ-alumina and kaolinite was proposed to occur as outer sphere complexes (He et al. 1997). On soils, it was described as inner sphere complexation, which was correlated with the soil iron oxide content (Kooner et al. 1995), which was in agreement with hematite oxide results (Eggleston et al. 1998). Adsorption of sulfate on mineral clays was assigned to the formation of inner sphere complex through one surface site or through a bridge complex (Sarbak 1994).

The results obtained for the PCM adsorption on P0.5 sample in the presence of different anions indicated competition on the adsorption sites when phosphate or sulfate was present. PCM adsorption on raw and PILC minerals was reported to occur by the formation of inner sphere complexes between PCM molecules and the mineral surface through the interaction of the carboxylic and pyridine nitrogen moieties of PCM and the metal centers of the pillars on the mineral surface
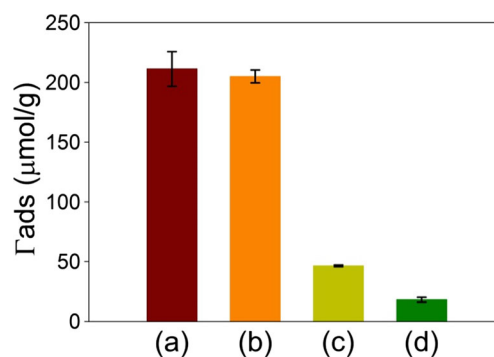

Fig. 5 PCM adsorption on P0.5 sample in the absence (*a*) or in the presence of the anions chloride (*b*), sulfate (*c*), and phosphate (*d*). The molar ratio used was 1:1

(Marco-Brown et al. 2014; Marco-Brown et al. 2012; Marco-Brown et al. 2015). Therefore, these results are consistent with a PCM adsorption onto the surface of the PILC by forming an inner sphere complex with the metal centers of silicon, aluminum, or iron.

A FTIR study was carried out in order to get an insight into the mechanisms that operate in the preparation of SRFs.

FTIR analysis

The FTIR spectra of PCM, HPβ, P0.5, PCM-P0.5, PCM-HPβ, PCM-HPβ(PM), and PCM-HPβ-P0.5 are shown in Figs. 6 and 7. The band assignations of PCM, HPβ, and P0.5 are listed in Tables 3 and 4.

Interaction between PCM and P0.5 (PCM-P0.5 sample)

The band of PCM at 1706 cm^{-1} was not present, which indicated that protonated carboxylic form of PCM was absent in PCM-P0.5 sample. The PCM band at 1600 cm^{-1} shifted to 1623 cm^{-1}, which revealed interaction of PCM carboxylic group with the surface. The band of PILC at 1635 cm^{-1} corresponding to interlayer water disappeared or diminished its intensity due to PCM entrance into the clay galleries and the exit of surface water. The band of PCM at 1456 cm^{-1} corresponding to C═C pyridine ring stretching vibrations shifted to 1427 cm^{-1} in the adsorbed sample, which confirmed the PCM interaction with clay surface through pyridine nitrogen. The
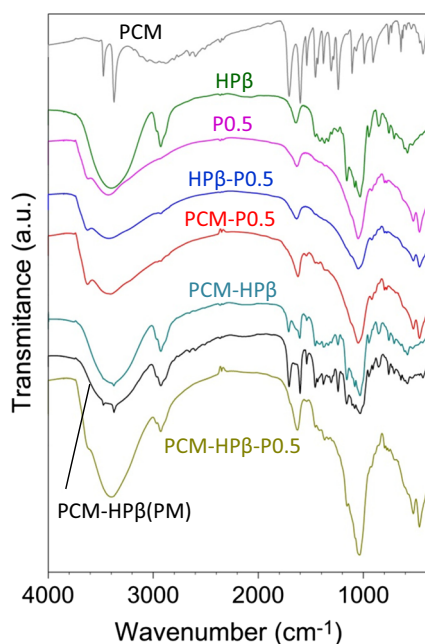

Fig. 7 FTIR spectra of PCM (*gray*), HPβ (*green*), P0.5 (*violet*), HPβ-P0.5 (*blue*), PCM-P0.5 (*red*), PCM-HPβ (*blue green*), PCM-HPβ(PM) (*black*), and PCM-HPβ-P0.5 (*moss green*) samples. Spectral region evaluated from 400 to 1800 cm^{-1}
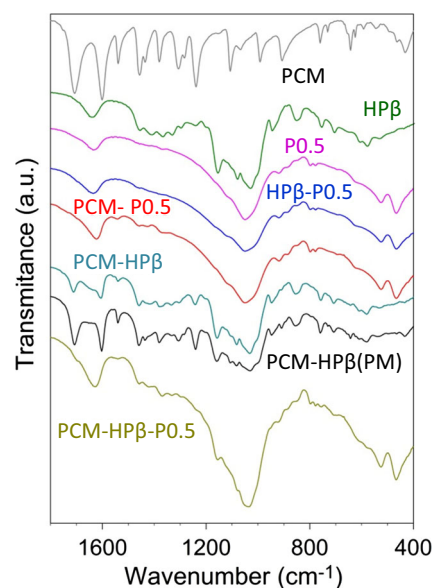
band of PCM at 1381 cm^{-1} assigned to symmetric stretching vibration of the dissociated carboxyl group shifted to 1367 cm^{-1} due to PCM interaction through its carboxylic group with the clay surface. All these shifts could be attributed to the interaction of the PCM with the solid surface by formation of a monodentate or bidentate coordination that involves the COO$^-$ group and the nitrogen of the pyridine ring as previously suggested for picolinic acid interactions with Al(III)-(hydr)oxide minerals (Loring et al. 2000).

PCM-HPβ complex

The bands of PCM at 1706, 1600, 1238, and 906 cm^{-1} corresponded to C═O stretching vibrations, COO$^-$ stretching, and N–H bending vibrations, to C–N stretching vibrations and to N–H wagging vibrations, respectively. These bands shifted to 1711, 1605, 1242, and 911 cm^{-1}, respectively, in the PCM-HPβ complex due to PCM interactions with the CD. The bands of PCM at 1456, 1066, 991, 760, and 731 cm^{-1} overlapped with CD bands. All the remaining bands of PCM were visible in the PCM-HPβ spectrum. As expected, an interaction between PCM and HPβ occurred when both were present in the aqueous solution, where PCM was located partly in the hydrophobic cavity of HPβ.

HPβ-P0.5 sample

HPβ bands at 854, 1032, and 2929 cm^{-1} appeared in HPβ-P0.5 sample, which indicated the absence of HPβ interaction

Fig. 6 FTIR spectra of PCM (*gray*), HPβ (*green*), P0.5 (*violet*), HPβ-P0.5 (*blue*), PCM-P0.5 (*red*), PCM-HPβ (*blue green*), PCM-HPβ(PM) (*black*), and PCM-HPβ-P0.5 (*moss green*) samples. Spectral region evaluated from 400 to 4000 cm^{-1}

Table 3 Group assignations to the mean FTIR peaks of PCM, HPβ, and P0.5 samples

Sample	Band (cm^{-1})	Assignment
PCM	3475	N–H stretching
	3373	N–H stretching
	1706	C=O stretching
	1600	COO$^-$ stretching and N–H bending
	1539	C=N pyridine ring stretching
	1456	C=C pyridine ring stretching
	1435	C=C pyridine ring stretching
	1381	COO$^-$ stretching
	1306	C–Cl in-plane bending
	1284	C–Cl in-plane bending
	1238	C–N stretching
	1107	C–Cl in-plane bending
	1066	C–Cl in-plane bending
	991	C–Cl out-of-plane bending
	906	N–H wagging
	760	C–Cl stretching
	731	C–Cl stretching
HPβ	3398	O–H stretching
	2929	CH$_2$ stretching
	1645	H–O–H bending
	1458	C–H bending from CH$_2$ and CH$_3$
	1412	C–H bending from CH$_2$ and CH$_3$
	1369	C–H bending from CH$_3$
	1334	C–C–H and C–O–H bending H–C–H bending
	1300	C–H in-plane bending
	1244	C–H in-plane bending
	1201	C–H in-plane bending
	1157	C–O–C stretching/O–H bending
	1082	Coupled C–O/C–C stretching/O–H bending
	1032	Coupled C–O/C–C stretching/O–H bending
	947	C–H out-of-plane bending
	854	C–H out-of-plane bending
	756	C–H wagging
	708	C–H wagging

Table 4 Group assignations to the mean FTIR peaks of P0.5 sample

Sample	Band (cm^{-1})	Assignment
P0.5	3612	O–H stretching vibration
	3420	O–H stretching vibration
	1635	Interlayer water
	1049	In-plane Si–O–Si stretching vibration
	920	Al–Al–OH deformation
	890	Si–O vibrations of some quartz impurities of the raw mineral
	797	Si–O vibrations of quartz
	777	Si–O vibrations of quartz

PCM adsorbed on P0.5 surface in presence of HPβ (PCM-HPβ-P0.5 sample)

The shifts of the absorption bands observed are similar to those observed with the PCM-P0.5 sample. The bands of PCM at 1706 and 1600 cm^{-1} corresponding to C=O stretching vibrations and COO$^-$ stretching which shifted to 1698 (shoulder) and 1623 cm^{-1}, respectively, indicating interaction of PCM carboxylic group with the surface. The band of PCM at 1456 cm^{-1}, which corresponded to C=C pyridine ring stretching vibrations shifted to 1427 cm^{-1} confirming an interaction of PCM with mineral surface through its pyridine nitrogen. The band of PCM at 1381 cm^{-1} was assigned to symmetric stretching vibration of the dissociated carboxyl group shifted to 1367 cm^{-1} due to PCM interaction through carboxylic group with clay surface groups. These results are in agreement with the formation of an inner sphere complex through a bidentate interaction. The absence of any shift in the HPβ bands at 1412, 1333, 1300, 1157, 1082, 947, 754, and 704 cm^{-1} in PCM-HPβ-P0.5 sample indicated no interaction between HPβ and the clay surface, as stated previously. This behavior was also supported by the analysis of PCM adsorption in the presence/absence of HPβ by the Langmuir model and in line with findings of Jozefaciuk et al. (Jozefaciuk et al. 2001), who reported a very low affinity with the clay surface. This behavior supported the previous PCM adsorptions results where there was no difference between PCM adsorptions in the presence or absence of HPβ.

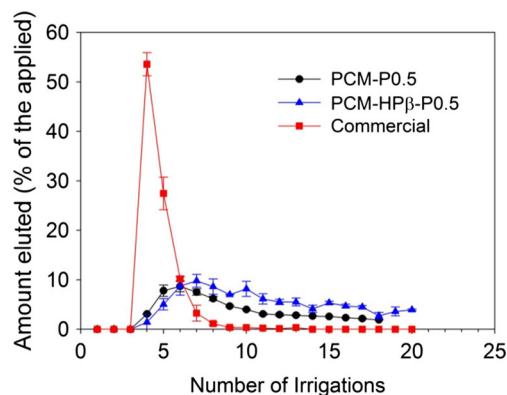## Physical mixture of PCM and HPβ (PCM-HPβ(PM) sample)

As expected, the FTIR spectrum of the PCM and CD physical mixture was the sum of the separate IR spectrums of PCM and CD. The absence of absorption peak shifts indicated no interaction between both molecules when mixed physically.

Fig. 8 Herbicide release from the commercial and PCM-clay formulations

between HPβ and clay surfaces. These results indicated PCM adsorption in the absence of PCM-HPβ complex on the clay surface. On the one hand, the presence of HPβ contributed to increase the PCM concentration in solution, and on the other hand, the great affinity of PCM with the clay surface together with the low apparent stability constant of the PCM-HPβ complex resulted in the rupture of the complex, thus increasing PCM loading on the clay surface.

Summarizing, the interaction between PCM and HPβ molecules was established by FTIR analyses. The interaction absence between HPβ and pillared mineral surface was also confirmed from the adsorption study. FTIR results indicated that, even in the presence or absence of HPβ, PCM interacted with clay surface sites through its carboxylic and pyridine nitrogen groups.

Release studies

PCM elution tests were made on a SS by adding the PCM-P0.5 and PCM-HPβ-P0.5 SRFs, and the results were compared to those of a commercial solution applied at same rate. PCM concentration, expressed as % of PCM applied, in the eluates after 20 consecutive irrigation steps with water is shown in Fig. 8. The commercial formulation showed a sharp peak indicative of a very rapid elution of PCM with almost negligible retention in this soil. On the contrary, the released amounts with the pillared clay formulations showed flattened peaks consistent with a gradual release of the active ingredient.

After 13 irrigation steps, the commercial formulation eluted completely ($97.0 \pm 8.2\%$), whereas the total recoveries were $70.1 \pm 12.1\%$ for PCM-HPB-0.5 and $76.9 \pm 9.8\%$ for PCM-P0.5 samples, respectively, amounting to a total reduction of releases of 28 and 22%, respectively. The curves for the PILC-based formulations were quite close to each other in agreement with the same mechanism of retention (electrostatic interactions with the pillars); the only difference between them was the higher a.i. content on PCM-HPB-0.5 (19% in excess).

Conclusions

PILC mineral was synthesized varying the Fe/(Fe + Al) molar ratio in order to design SRF of the herbicide PCM based on the high affinity of PCM observed with iron oxide surfaces. Therefore, an enhanced adsorption of PCM on iron modified clay and a slow release of it were achieved. The P0.5 sample evidenced a higher adsorption capacity of PCM than that found for P0.15 sample.

An increase in the loading of PCM on samples was achieved by using CDs as solubilizing agent due to the formation of inclusion complexes. The use of these complexes increased the amount of PCM adsorbed on the PILC. The use of HPβ in the preparation of PCM-Al–Fe PILC formulations is recommended for the slow release of PCM.

The interaction between PCM and HPβ molecules was established by FTIR analyses. It was confirmed a lack of interaction between HPβ and pillared mineral surface from the adsorption study. FTIR results suggested that PCM interacted with clay surface sites through its carboxylic and pyridine nitrogen groups. Competitive adsorption of anions confirmed an inner sphere complexation between PCM and clay surface. Release of the herbicide in a SS from PCM-clay formulations was retarded compared to the commercial formulation Tordon® 101.

References

Akelah A (1996) Novel utilizations of conventional agrochemicals by controlled release formulations. Mater Sci Eng C 4:83–98

Ali I, Asim M, Khan TA (2012) Low cost adsorbents for the removal of organic pollutants from wastewater. J Environ Manag 113:170–183

Alromeed AA, Scrano L, Bufo SA, Undabeytia T (2015) Slow-release formulations of the herbicide MCPA by using clay-protein composites. Pest Manag Sci 71:1303–1310

Biggar JW, Mingelgrin U, Cheung MW (1978) Equilibrium and kinetics of adsorption of picloram and parathion with soils. J. Agr. Food Chem. 26:1306–1312

Campos EVR, de Oliveira JL, Fraceto LF, Singh B (2014) Polysaccharides as safer release systems for agrochemicals. Agron Sustain Dev 35:47–66

Carrizosa MJ, Calderón MJ, Hermosín MC, Cornejo J (2000) Organosmectites as sorbent and carrier of the herbicide bentazone. Sci Total Environ 247:285–293

Celis R, Hermosin MC, Cornejo L, Carrizosa MJ, Cornejo J (2002) Clay-herbicide complexes to retard picloram leaching in soil. Int J Environ An Ch 82:503–517

Cheung MW, Biggar JW (1974) Solubility and molecular-structure of 4-amino-3,5,6-trichloropicolinic acid in relation to pH and temperature. J. Agr. Food Chem. 22:202–206

Delcour I, Spanoghe P, Uyttendaele M (2015) Literature review: impact of climate change on pesticide use. Food Res Int 68:7–15

Eggleston CM, Hug S, Stumm W, Sulzberger B, dos Santos AM (1998) Surface complexation of sulfate by hematite surfaces: FTIR and STM observations. Geochim. Cosmochim. Ac. 62:585–593

Entry JA, Sojka RE (2008) Matrix based fertilizers reduce nitrogen and phosphorus leaching in three soils. J Environ Manag 87:364–372

Essington ME (2004) Soil and water chemistry, an integrative approach. CRC Press, Boca Raton

FAO FaAOotUN (2007): Specifications and evaluations for agricultural pesticides, Picloram. http://www.fao.org

Galán-Jiménez MC, Mishael YG, Nir S, Morillo E, Undabeytia T (2013) Factors affecting the design of slow release formulations of

herbicides based on clay-surfactant systems. A Methodological Approach PLoS ONE 8:e59060

Gupta VK, Suhas (2009) Application of low-cost adsorbents for dye removal—a review. J Environ Manag 90:2313–2342

Hall KE, Ray C, Ki SJ, Spokas KA, Koskinen WC (2015) Pesticide sorption and leaching potential on three Hawaiian soils. J Environ Manag 159:227–234

Haynes D, Müller J, Carter S (2000) Pesticide and herbicide residues in sediments and seagrasses from the Great Barrier Reef World Heritage Area and Queensland Coast. Mar Pollut Bull 41:279–287

He LM, Zelazny LW, Baligar VC, Ritchey KD, Martens DC (1997) Ionic strength effects on sulfate and phosphate adsorption on γ-alumina and kaolinite: triple-layer model. Soil Sci Soc Am J 61:784–793

Higuchi T, Connors K (1965) Phase solubility techniques. In: Reilly CN (ed) Advances in analytical chemistry instrumentation. Interscience, New York, NY, pp 117–212

Jozefaciuk G, Muranyi A, Fenyvesi E (2001) Effect of cyclodextrins on surface and pore properties of soil clay minerals. Environ. Sci. Technol. 35:4947–4952

Kashyap PL, Xiang X, Heiden P (2015) Chitosan nanoparticle based delivery systems for sustainable agriculture. Int J Biol Macromol 77:36–51

Kenawy ER, Sherrington DC, Akelah A (1992) Controlled release of agrochemical molecules chemically bound to polymers. Eur Polym J 28:841–862

Kooner ZS, Jardine PM, Feldman S (1995) Competitive surface complexation reactions of sulfate and natural organic carbon on soil. J Environ Qual 24:656–662

Lagaly G (2001) Pesticide-clay interactions and formulations. Appl Clay Sci 18:205–209

Loewy M, Kirs V, Carvajal G, Venturino A, Pechen De D'Angelo AM (1999) Groundwater contamination by azinphos methyl in the Northern Patagonic Region (Argentina). Sci Total Environ 225:211–218

Loring JS, Karlsson M, Fawcett WR, Casey WH (2000) Attenuated total reflection-Fourier-transform infrared and 27 Al-nuclear magnetic resonance investigation of speciation and complexation in aqueous Al(III)-picolinate solutions. Geochim Cosmochim Ac 64:4115–4129

Maqueda C, Villaverde J, Sopeña F, Undabeytia T, Morillo E (2008) Novel system for reducing leaching of the herbicide metribuzin using clay-gel-based formulations. J. Agr. Food Chem. 56:11941–11946

Maqueda C, Villaverde J, Sopeña F, Undabeytia T, Morillo E (2009) Effects of soil characteristics on metribuzin dissipation using clay-gel-based formulations. J. Agr. Food Chem. 57:3273–3278

Marco-Brown JL, Barbosa-Lema CM, Torres Sánchez RM, Mercader RC, dos Santos AM (2012) Adsorption of picloram herbicide on iron oxide pillared montmorillonite. Appl Clay Sci 58:25–33

Marco-Brown JL, Areco MM, Torres Sánchez RM, dos Santos AM (2014) Adsorption of picloram herbicide on montmorillonite: kinetic and equilibrium studies. Colloid Surface A 449:121–128

Marco-Brown JL, Trinelli MA, Gaigneaux EM, Torres Sánchez RM, Dos Santos AM (2015) New insights on the structure of the picloram-montmorillonite surface complexes. J Colloid Interf Sci 444:115–122

Mishra T, Mohapatra P, Parida KM (2008) Synthesis, characterisation and catalytic evaluation of iron-manganese mixed oxide pillared clay for VOC decomposition reaction. Appl Catal, B 79:279–285

Morillo E, Sánchez-Trujillo MA, Villaverde J, Madrid F, Undabeytia T (2014) Effect of contact time and the use of hydroxypropyl-β-cyclodextrin in the removal of fluorene and fluoranthene from contaminated soils. Sci Total Environ 496:144–154

Nir S, Undabeytia T, Yaron-Marcovich D, El-Nahhal Y, Polubesova T, Serban C, Rytwo G, Lagaly G, Rubin B (2000) Optimization of adsorption of hydrophobic herbicides on montmorillonite preadsorbed by monovalent organic cations: interaction between phenyl rings. Environ Sci Technol 34:1269–1274

Osteryoung J, Whittaker JW (1980) Picloram—solubility and acid-base equilibria determined by normal pulse polarography. J. Agr. Food Chem. 28:95–97

Palma G, Sanchez A, Olave Y, Encina F, Palma R, Barra R (2004) Pesticide levels in surface waters in an agricultural-forestry basin in Southern Chile. Chemosphere 57:763–770

Pérez-Martínez JI, Ginés JM, Morillo E, Moyano JR (2000) 1H-nuclear magnetic resonance and phase solubility studies of the stoichiometries in 2,4-D: α-and β-cyclodextrins inclusion complexes. J Inclusion Phenom 37:171–178

Qi Y, Donahoe RJ (2008) The environmental fate of arsenic in surface soil contaminated by historical herbicide application. Sci Total Environ 405:246–254

Sánchez-Jiménez N, Sevilla MT, Cuevas J, Rodríguez M, Procopio JR (2012) Interaction of organic contaminants with natural clay type geosorbents: potential use as geologic barrier in urban landfill. J Environ Manag 95:Supplement:S182–Supplement:S187

Sarbak Z (1994) Structural and surface properties of anion-activated clay. Mater Chem Phys 39:91–97

Schipper PNM, Vissers MJM, van der Linden AMA (2008): Pesticides in groundwater and drinking water wells: overview of the situation in the Netherlands, Water Science and Technology, pp. 1277–1286

Szejtli J (1998) Introduction and general overview of cyclodextrin chemistry. Chem Rev 98:1743–1753

Undabeytia T, Sopeña F, Sánchez-Verdejo T, Villaverde J, Nir S, Morillo E, Maqueda C (2010) Performance of slow-release formulations of alachlor. Soil Sci Soc Am J 74:898–905

Undabeytia T, Recio E, Maqueda C, Morillo E, Gómez-Pantoja E, Sánchez-Verdejo T (2011) Reduced metribuzin pollution with phosphatidylcholine-clay formulations. Pest Manag Sci 67:271–278

Undabeytia T, Recio E, Maqueda C, Sánchez-Verdejo T, Balek V (2012) Slow diuron release formulations based on clay-phosphatidylcholine complexes. Appl Clay Sci 55:53–61

Undabeytia T, Galán-Jiménez MC, Gómez-Pantoja E, Vázquez J, Casal B, Bergaya F, Morillo E (2013) Fe-pillared clay mineral-based formulations of imazaquin for reduced leaching in soil. Appl Clay Sci 80-81:382–389

Wang Y, Gao Z, Shen F, Li Y, Zhang S, Ren X, Hu S (2015) Physicochemical characteristics and slow release performances of chlorpyrifos encapsulated by poly(butyl acrylate- co -styrene) with the cross-linker ethylene glycol dimethacrylate. J Agr Food Chem 63:5196–5204

Wenz G, Han BH, Müller A (2006) Cyclodextrin rotaxanes and polyrotaxanes. Chem Rev 106:782–817

Yan H, Chen X, Feng Y, Xiang F, Li J, Shi Z, Wang X, Lin Q (2015) Modification of montmorillonite by ball-milling method for immobilization and delivery of acetamiprid based on alginate/exfoliated montmorillonite nanocomposite. Polym Bull 73:1185–1206

Yáñez C, Cañete-Rosales P, Castillo JP, Catalán N, Undabeytia T, Morillo E (2012) Cyclodextrin inclusion complex to improve physicochemical properties of herbicide bentazon: exploring better formulations. PLoS One 7:e41072